THE HAZARDS POSED BY LARGE-SCALE POOL FIRES IN OFFSHORE PLATFORMS

G.A.Chamberlain
Shell Research Ltd., Thornton Research Centre, P.O.Box 1, Chester, U.K., CH1 3SH

An experimental programme of large-scale diesel pool fires has been carried out to obtain an understanding of the behaviour of pool fires in degrees of confinement representative of offshore modules, and simultaneously to provide benchmark data against which compartment pool fire models can be validated. The test compartment was a 135 m^3 insulated steel rig with variable ventilation at the Norwegian Fire Laboratory operated by SINTEF, Trondheim. Data on heat fluxes, temperature, burning rate, and combustion product concentrations were obtained during fire development to quasi-steady state under different ventilation conditions. Fire severity is similar to that of jet fires, except that it is worst in *over*-ventilated, but confined conditions. The results are compared with predictions of global stoichiometry to demonstrate the validity and limitations of a zone modelling approach, which is then used as a basis for guidance on the hazard severity.

Key Words: compartment pool fires; offshore platform safety.

INTRODUCTION

The hazards posed by accidental pool fires are an important aspect of Safety Cases prepared for offshore platforms. However, there is considerable uncertainty, Cowley [1], in the extent of the fire severity and the effectiveness of typical deluge systems in mitigating the hazards. Consequently a major programme of compartment fire research, Chamberlain [2], [3], has been carried out by Shell Research Ltd at the Norwegian Fire Laboratory operated by SINTEF at Trondheim. This paper reports novel results on the behaviour of large-scale hydrocarbon pool fires in confined surroundings, typical of offshore modules, under carefully monitored conditions of temperature, vent flow, heat flux and product concentrations.

Whilst the scale was chosen to be representative of offshore modules, it also presented an opportunity to investigate the extent of enhanced radiative feedback to the pool surface in increasing the burning rate, an effect often reported at smaller scale. Previous research has also demonstrated the strong link between the global stoichiometry of the fire (defined as the ratio of the stoichiometric air requirement to the actual air entrained into the compartment) and, *inter alia*, combustion product concentrations, Beyler [4]. Thus, the implications for the offshore hazards are analysed in terms of correlations between global stoichiometry of compartment pool fires approaching steady state and fire intensity.

EXPERIMENTAL PROCEDURE

Details of the pool fire layout, compartment geometry and design, and instrumentation are described in detail in references 2 and 3, and only a brief summary is given here. A diagram of the apparatus and instrument locations is shown in Figure 1. The compartment was 135m^3 in volume, 3.91m high, 3.54m wide and 9.8m long, and had fully insulated walls lined internally with 1mm thick stainless steel sheet. One of the smaller end walls was vented with an area of 2m x 2.5m (height x width) for ventilation control and a fully open wall for fuel controlled flames. The 2mm thick steel plate restricting the vent opening was not insulated. Experimental conditions are summarised in Table 1.

TABLE 1. Summary of Compartment Pool Fire Experiments.

Test no.	ool area m^2	Number of pans	ool location	Vent size (ht x w) m	Vent location	eluge yes/n
23	3 x 2	6	central	4 x 3.5	end wall	no
25	3 x 2	6	central	2 x 2.5	end wall	no
26	3 x 2	6	central	2 x 2.5	end wall	yes
24	3 x 4	12	central	4 x 3.5	end wall	no
22	3 x 2	6	east wall	long x 2.5 wid	oof - off centre	no

The fuel was Shell Commercial Grade diesel and was burnt in $1m^2$ steel pans over a 50mm water layer, located centrally in the compartment with side venting and located at the east end when the venting was in the roof. In each experiment 20kg of fuel was loaded into each pan. Samples analysed at Thornton revealed a large range of both aromatic and paraffinic components from C5 to C25 with a peak at around C15 to C20 and boiling in the range 165-360^oC. A calibration test using one pan and 8.12 litres of fuel had an overall burning rate of 0.03 $kg/m^2/s$. This is about 50% of the burning rate of kerosene (C11-C16) in large pool fires on land, but is representative of the burning rate of crude oil, Babrauskas [5].

An attempt was made to measure directly the rate of fuel mass loss rate (or burning rate) by placing a load cell under one of the central pans. Unfortunately, equivocal results were always obtained and interpretation remains unclear. Thus, the only measure of burning rate is the less informative one derived from the total time to a marked drop in fire intensity due to fuel depletion.

Pool fires with side ventilation were located directly beneath a target instrumented with 4 total heat flux gauges, 2 ellipsoidal radiometers and 12 thermocouples. One ellipsoidal radiometer was located in the centre of one pan, 378mm above the pool surface and viewing directly upwards, to monitor radiative feedback to the pool. As in previous experiments with jet fires the compartment was fully instrumented with thermocouples in the internal gas volume, roof, walls and vent. Heat flux gauges were located in the end wall and roof. Note that the heat flux gauges were maintained at a constant 55$\pm$5^oC throughout the measuring period, so the values represent the initial heat flux that would be incident on an ambient temperature object placed at that position in the flame. Vent flows were monitored by differential pressure probes and thermocouples in the vent plane. Combustion products (CO, CO_2, O_2 and soot) concentrations in the plume emerging from the compartment were measured as before [3].

A deluge system consisting of 4 medium velocity nozzles spaced at 2m intervals and delivering nominally 10 litres/m^2/min was installed in the ceiling for experiment 26. This system was designed to be representative of offshore practice, and further details are given in reference 3.

RESULTS

Five pool fire experiments (designated "22-26") were carried out, of which 4 were side-vented to explore the variation of ventilation and pool fire size and the effect of deluge, and the other was roof ventilated. A summary of the main results is shown in Table 2.

TABLE 2. Summary of Temperature and Heat Flux Data. The average maximum radiation in the roof is derived from radiometer measurements at 3.85m from the east wall on the roof centre line. The fluctuations in signal, and hence in heat flux, are typically of the order of ±12%.

Test no.	Time to burn out,s	Mass loss rate, $kg/m^2/s$	Maximum gas temperatures, ^oC				Max. wall temps, ^oC		Max. roof temps, ^oC		Aver. max. roof radn kW/m^2
			East		West						
			top	bottom	top	bottom	top	bottom	centre	edge	
23	450	0.044	1100	750	> 1350		1150	1050	1200	950	240
25	650	0.031	1200	1100	1100	800	1020	820	1100	1100	200
26	N/A	-	50	100	50	100	80	70	310	240	N/A
24	450	0.044	1250	1250	1300	1300	1000	700	1300	1200	280
22	1050	0.019	800	1100	1000	700	950	700	1000	1100	160

Experiment 23 was carried out using a pool area of $6m^2$ in a well ventilated compartment. The fire behaved as if totally unconfined, except in the later stages, when effects arising from the hot compartment became evident. Initially however, copious amounts of smoke were generated and for the first 90 seconds flames were confined to the compartment, indicating that burning was fuel controlled. Product and air velocities, and hence mass flows, derived from measurements of differential pressure and temperature at the vent also confirmed that combustion was fuel controlled.

After about 300 seconds the fire reached a quasi-steady state and the internal gas temperatures peaked, see Figure 2. Flames extended about 2m from the top of the vent, considerably longer than would be predicted from the correlation given in You and Faeth [6]. A mass influx of air of 9.7±20% kg/s was derived from an average peak vent velocity of 1.5m/s and derived vent discharge coefficient of 0.7, over an area of width 3.5m and height 2.2m to the air/smoke interface (or neutral plane). Air entrainment of about 15 times the mass loss rate is required for global stoichiometric combustion, so the actual global stoichiometry ϕ in this experiment was 0.4±25%. A similar calculation based on the mass outflow gave a ϕ of 0.42±30% after correcting for the mass rate of fuel loss (see Table 3). This result is less accurate because fewer measurements of differential pressure and temperature were taken in this experiment in the smoke layer at the vent. Although the air entrainment is about 2.5 times greater than the stoichiometric requirement it is still considerably less than the amount associated with a truly open flame, Delichatsios [7]. The fire should perhaps be more correctly regarded as quasi-ventilation controlled rather than fuel controlled, and partly explains why a limited amount of combustion occurred outside the opening.

TABLE 3. Vent flows and global stoichiometries derived from experimental data compared with calculated results; v is gas velocity at the vent, where subscript a is air and subscript o is outflowing gases, subscript max is the average maximum; m is mass flow, where subscript f is fuel; z_n is the height of the neutral plane above the floor of the rig, and ϕ is the global stoichiometry. The estimated accuracy on experimentally derived values of ϕ is $\pm$25% (but see text).

Test	Inflow				Outflow				Calculated results		
no.	v_{amax} m/s	m_a kg/s	z_n m	ϕ	v_{omax} m/s	m_o kg/s	m_o-m_f kg/s	ϕ	m_a kg/s	z_n m	ϕ
23	1.5	9.7	2.2	0.4	8.5	10.0	9.8	0.42	8.0	2.3	0.5
25	1.2	2.5	1.0	1.1	5.8	2.46	2.3	1.2	2.3	1.1	1.3
24	2.1	11.7	1.9	0.7	9.5	11.6	11.1	0.72	9.4	2.1	0.9

The burning rate in Table 2 was greater than that measured in the calibration test using one pan but was the same as that for 12 pans in the same compartment geometry (test 24), and probably represents an upper limit for the mass burning rate for this fuel. Interestingly, the pan radiometer measured constant average radiation throughout the burn period and showed no evidence for enhanced burning due to increased radiative feedback from the hot surroundings, a phenomenon which is often reported at smaller scale. These results strongly suggest that the mechanism of radiative feedback which controls the burning rate had maximised, and that the fire had attained its peak value of fuel loss rate.

A remarkable feature of this experiment was the extremely high temperatures generated in the upper portion of the fire plume in the later stages, see Figure 3. The west and south thermocouples recorded temperatures in excess of 1350^{o}C before failing and eventually melting, and a total heat flux of 310$\pm$20 kW/m^2 was recorded in the middle of the end wall, see Figure 4. The heat flux in the roof directly above the pool peaked at 240$\pm$30 kW/m^2 as recorded by both radiometer and nearby total heat flux gauge, indicating the total dominance of radiation over convective heat flux. The results also show that internal heat fluxes commonly associated with pool fires in the open [1] are readily exceeded once the fire is confined by insulated boundaries.

These high temperatures were associated with a sudden increase in soot concentration, see Figure 5. We hypothesise that unburnt fuel in the fire plume is pyrolysed to soot more readily at these higher temperatures, and in the hot surroundings the normal radiative losses from soot particles become less efficient than in a pool fire in the open due to re-absorption of radiation from the compartment boundaries. Thereafter, the soot concentration dropped markedly. The upper limit on soot concentration is determined by the balance between the rates of formation and destruction. In this experiment there is excess air and the local conditions favour the soot particles remaining hot enough for long enough to oxidise more readily than in a totally unconfined flame. It is thought that the burning soot contributes to the visible flame length and further explains why the correlation in reference 6 under-predicts the ceiling jet flame length. The fact that the carbon dioxide concentration shown in Figure 6 increased by up to 1.5%v and the oxygen concentration decreased by about 2.5%v during this period supports this idea. Thus, at quasi-steady state, the compartment temperature, associated heat flux, and soot concentration are intimately dependent on the global stoichiometry and the degree of insulation at the compartment boundaries. Heat losses from a non-insulated compartment would become increasingly significant with temperature rise resulting in lower internal temperatures and heat flux, but greater amounts of smoke.

In experiment 25 the pool area and fuel loading were identical to those of 23 but the ventilation opening was reduced from $14m^2$ to $5m^2$. Initially the fire consumed the air in the compartment and large amounts of smoke emerged from the vent. After 103 seconds a small external flame appeared in the smoke at the vent. At 150 seconds after ignition smoke production suddenly increased significantly (see Figure 7), coincident with the carbon dioxide concentration reaching a maximum of 14%v and the oxygen concentration falling to near zero, see Figure 8. At this stage the fire was fully ventilation controlled. Thereafter the fire continued to burn at constant intensity for a total duration of about 650 seconds giving an overall burning rate of 0.031 kg/m2/s, considerably less than the fuel controlled fire in test 23. Gas volume temperatures and radiative heat flux directly in the fire plume (Figure 9) were also lower than in test 23, although the hot upper layer extended further down the compartment resulting in higher temperatures outside the main fire plume (see Table 2). One notable feature was the uniformity of gas temperature (1100-1200^{o}C) in this upper layer (Figure 10).

Measurements of differential pressures and temperatures at the vent indicated that at quasi-steady state the fire was burning in the near stoichiometric but slightly under-ventilated regime; $\phi \approx 1.15$ (see Table 3). It would appear that the burning rate becomes limited by the reduced radiative feedback from a partially combusted, and hence cooler, fire plume. The flame stoichiometry stabilises in the regime in which the burning rate is maximised for the particular pool size and compartment geometry under investigation.

When deluge was applied to this fire, experiment 26, the burning rate was significantly reduced and the temperatures of the entire compartment and target decreased, see Figure 11. The fire was not extinguished but was successfully controlled. After an initial transient increase in burning rate caused by explosive boiling of the water droplets falling into the burning pool, the compartment volume temperature dropped rapidly to about 100^{o}C and the burning rate settled to a new, reduced, steady level. The oxygen concentration in the outflowing gases rose from near zero to about 18%v indicating that combustion had become fuel controlled. The external flame disappeared to be replaced by smoke.

Experiment 22 involved roof venting using an opening of the same dimensions as in 25. The vent was located in the west end of the roof, one metre away from the west wall. The average burning rate was considerably less than in test 25, as combustion became hindered by the competition between outflowing smoke and incoming air at the vent. Nevertheless, burning was sustained until fuel exhaustion, in contrast to flame extinction in identical geometry with a propane jet fire [2]. Carbon monoxide concentrations in the initially non-combusting smoke were slightly greater than previously reaching about 0.5%v before ignition. The vent probes indicated that there was no consistent pattern to the flow of gases and it proved impossible to derive meaningful vent velocities and global stoichiometry.

DISCUSSION

When a fire burns inside a compartment such as an offshore module the combustion starts as though the fire were in the open. There is enough air already present to satisfy the stoichiometric requirement. The hot combustion products rise to the ceiling and spread out as a ceiling jet. There is a net outflow of material through the compartment openings as the gases heat up. After a short time a hot gas layer of combustion products builds up in the upper part of the compartment and starts to descend as gases continue to flow into it. A relatively well defined interface forms between the upper hot layer and cool air below. When this interface descends below an opening there is a sudden outflow of smoke, combustion products or flame. An equilibrium is soon established between the hot gases flowing out and the air required for combustion flowing in. This bi-directional flow is separated by a neutral plane, where it is assumed that no flow occurs. In reality there will be some turbulent mixing due to shear forces between the hot and cold layers. At steady state the upper portion of the flame enters the hot upper layer and is unable to burn as an open fire. The fire is then ventilation controlled. Air is entrained along the fire plume up to the interface. It is this steady condition that is often taken as the basis for zone models and is the simple modelling approach explored here.

The fire product gases in the module are assumed to behave as if they are "well stirred", i.e. their properties are uniform throughout the volume, an assumption reasonably well supported by these experiments. These hot gases are assumed to leave the module above a neutral plane and cold air enters below it. The outflow of hot gases is assumed to be driven by buoyancy forces and the inflow of cold air is governed by the entrainment laws for induced buoyancy flows. No mixing is assumed between inflow and outflow.

Following Drysdale [8] and using the co-ordinate system shown in Figure 12, the mass rate of outflowing gases m_o for a single, vertical, rectangular vent at steady conditions is,

$$m_o = \frac{2}{3} C_d (2g\rho_g(\rho_a - \rho_g))^{1/2} y (z_l + H - z_n)^{3/2} \qquad (1)$$

where C_d is the vent discharge coefficient (0.7), g is gravity (9.81 ms^{-2}), ρ is density, subscript a refers to air and subscript g to the hot layer gases. In the experiments, $z_l = 0$, and $\rho_g \approx 0.24 kg/m^3$.

The mass flow of entrained air m_a is given by [7],

$$m_a = \frac{0.093 m_f}{Q^*} ((z_n - z_d)/d)^{3/2} F(F/(r+1))^{1/2} (\chi_a - \chi_r)^{1/2} \ , \ Q^* < 1 \qquad (2)$$

$$\text{where} \quad Q^* = m_f \Delta H / (\rho_a c_p T_a (gd)^{1/2} d^2) \qquad (3)$$

and m_f is the rate of fuel loss, ΔH is the net heat of combustion ($\approx$ 43MJ/kg), c_p is the heat capacity of air (1kJ/kg/K), T is temperature, d is the effective pool diameter, F is $\Delta H/c_p T_a$, r is the mass of air required for stoichiometric burning ($\approx$15.0), χ_a is the combustion efficiency and χ_r is the radiative fraction ($\chi_a - \chi_r \approx 0.6$).

By mass conservation,

$$m_o = m_a + m_f \qquad (4)$$

The equations can be solved for z_n, m_o and m_a by assigning appropriate values to the constants, and a value for the global stoichiometry ϕ (= rm_f/m_a) can be derived. A hot layer temperature of 1400K and composition equivalent to air have been used throughout. Note that the density term is not particularly sensitive to T_g; a change from 1400K to 1600K results in only a 5% difference in m_a.

The results of this analysis are compared with experimentally derived values in Table 3. In general the trends in data are well predicted, but the global stoichiometry is consistently slightly too high, i.e. the fire is predicted to be less ventilated than in reality. The origin of this mismatch could stem from the equation used to calculate the air entrainment rate, or more likely, it derives from the assumption that no mixing occurs in the shear layer at the interface between the cold lower layer and the hot upper product layer. Nevertheless, the calculation method can be recommended for first-order screening of fire scenarios, to determine whether combustion will be fuel- or ventilation-controlled and then to estimate the magnitude of the fire loading terms from the experimental results given here. Note however, that equation (1) for the outflow mass flux is only applicable to a single vertical vent. Flows through multiple openings at different levels must be calculated by more rigorous, but nonetheless simple, methods.

The correlation of the compartment pool fire stoichiometry with measured gas temperatures, heat fluxes and product concentrations is a useful concept but subject to the experimental conditions under which the data were obtained. In these experiments, for practical reasons, the compartment had a high degree of insulation, thereby minimising the heat loss during fire development. In a non-insulated module there would be significant heat loss from the boundaries and considerably lower temperatures, by several 100 degrees, could be expected, but the experiments do demonstrate that pool fire intensities of the same order as those of jet fires [2] can be reached. The results, therefore, could be regarded as representing an upper bound to the fire severity in a non-insulated module or applied directly to modules which are similarly insulated. Further experiments with reduced insulation are recommended.

Another approach would be to model fire development from the time of ignition, account for all the heat and mass transfer processes and calculate the fire loading terms as a function of time. Such methods have been attempted in the past [1] but all have suffered from lack of verification at the large scales representative of offshore modules. The present results could be used for such validation.

Some other words of caution are in order. The methodology described above will only predict the quasi-steady state value of ϕ and even then a product layer temperature must be assumed, although ϕ is not greatly sensitive to it. Also we observed that the fuel mass loss rate is dependent on ϕ when combustion becomes under-ventilated. The mass loss rate is difficult to calculate under compartment fire conditions but experimental values exist for many types of pool fires in the open, Cowley and Johnson [9], and an initial value based on these is recommended.

CONCLUSIONS

New results have been obtained on the behaviour of hydrocarbon pool fires in confined surroundings at a scale representative of offshore modules. The fire size was large enough to maximise the radiative feedback to the fuel surface, with the result that the overall burning rate was independent of fuel area. Fire severity, in terms of heat flux and gas temperatures in the fire plume, is shown to depend on natural ventilation rate but also appears to be a function of compartment temperature, which is in turn dependent on the degree of insulation of the compartment boundaries. The outcome in these experiments is that fire severity is worse in *over-*

ventilated, but confined conditions. The burning rate of ventilation controlled pool fires is self limiting and the fire tends to settle in the near stoichiometric, but slightly under-ventilated regime.

The roof ventilated fire examined here did not extinguish but continued to burn at much reduced rates. Similarly, application of water deluge in a manner typical of offshore practice did not extinguish the fire but reduced the burning rate significantly and effectively controlled the temperature of the surroundings.

Simple zone modelling is adequate to predict the (quasi-) steady state fire stoichiometry, but the development of the fire to this steady state requires a more sophisticated approach. Further experiments to investigate, for example, the effect of heat loss from the compartment boundaries and the location and size of pool on internal fire severity, are recommended.

ACKNOWLEDGEMENTS

The author wishes to thank: the staff at SINTEF NBL, Trondheim, for their co-operation and use of facilities, H.M.Brightwell and C.J.Townsend of Shell Research Ltd for their technical contributions, and Shell U.K./Esso U.K., the UK Health and Safety Executive, Shell Nederlands Aardolie Maatschappij and Norske Shell for their financial support and permission to publish.

REFERENCES

1. Cowley L.T., 1992, Offshore Technology Information, OTI 92 597 (HMSO Books, London).

2. Chamberlain G.A., "An experimental study of large scale compartment fires", Trans I.Chem.E., 72, Part B, Nov 1994, pp.211-219. Also presented at I.Chem.E. conference 'Hazards XII - European Advances in Process Safety', UMIST, Manchester, U.K., 19-21 April 1994, Symposium Series no.134.

3. Chamberlain G.A. and Brightwell H.M., "Large scale compartment fires, experimental data", U.K. Health and Safety Executive, Offshore Technology Series, OTO 94 011-024.

4. Beyler C.L., "Major species production by diffusion flames in a two-layer compartment fire environment", 1986, Fire Safety Journal, 10, 47-56.

5. Babrauskas V., "Burning Rates", 1988, SFPE Handbook of Fire Protection Engineering, Table 2-1.2, NFPA, Quincy MA.

6. You H.Z. and Faeth G.M., "Ceiling heat transfer during fire plume and fire impingement", Fire and Materials, 3, No.3, 140-147.

7. Delichatsios M.A., "Air entrainment into buoyant jet flames and pool fires", 1988, SFPE Handbook of Fire Protection Engineering, NFPA, Quincy MA.

8. Drysdale D., "An introduction to fire dynamics", 1985, J.Wiley and Sons Ltd, Chichester.

9. Cowley L.T. and Johnson A.D., 1992, Offshore Technology Information, OTI 92 596 (HMSO Books, London).

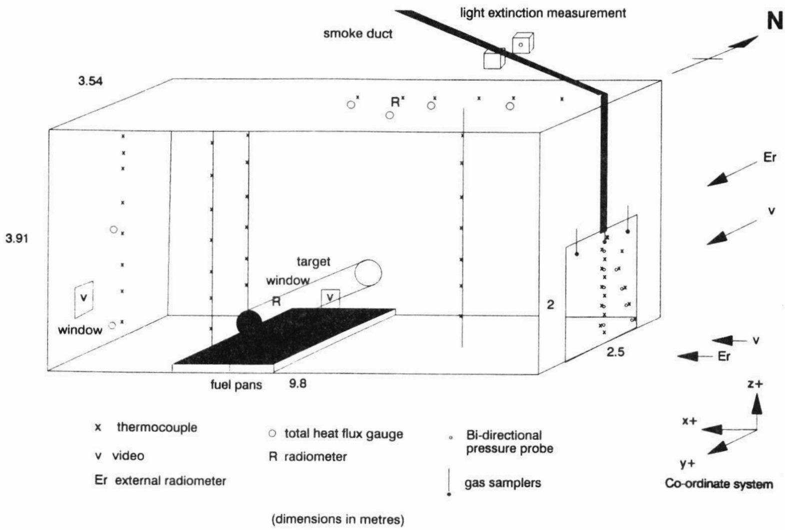

Figure 1. Typical compartment geometry and instrument locations.

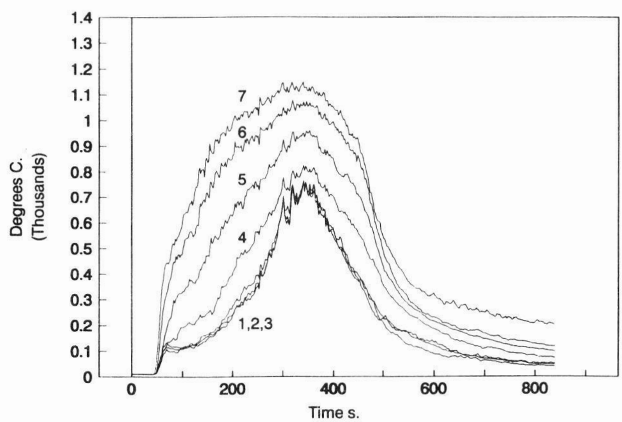

T/c no.	1	2	3	4	5	6	7
Height (m)	0.65	1.18	1.69	2.15	2.67	3.15	3.65

Figure 2. Test 23, temperatures at east thermocouple string.

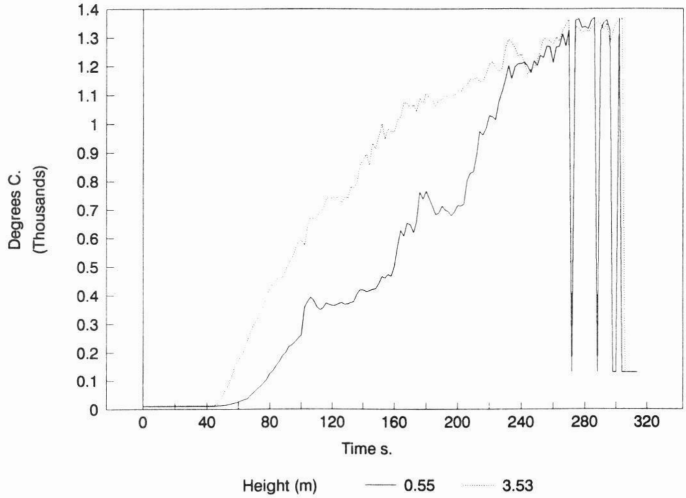

Figure 3. Test 23, temperatures at west thermocouple string up to moment of failure.

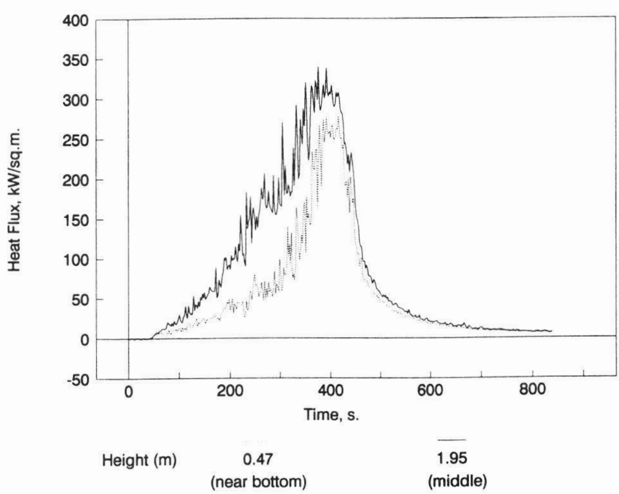

Figure 4. Test 23, total heat flux at west wall.

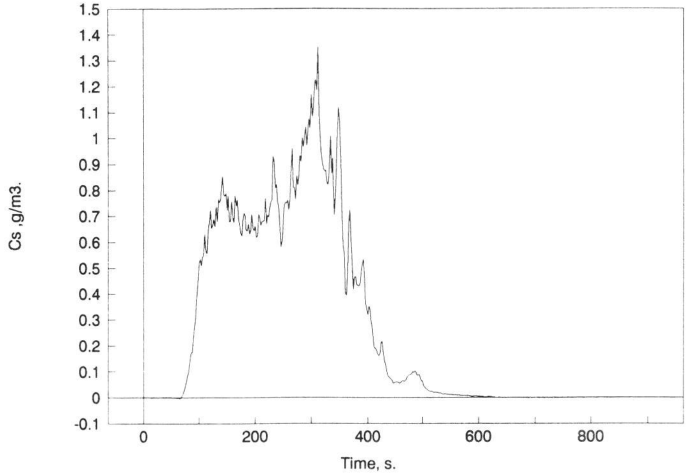

Figure 5. Test 23, derived soot concentration in the smoke at the vent.

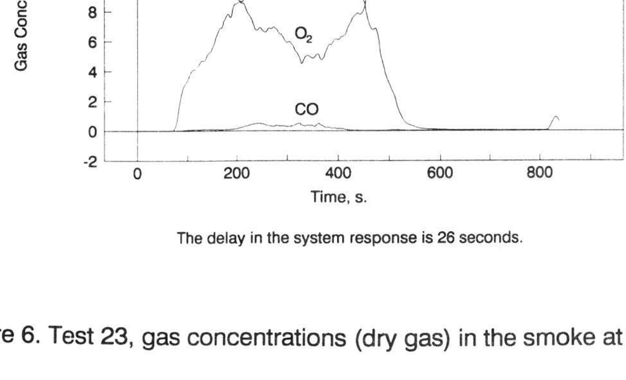

Figure 6. Test 23, gas concentrations (dry gas) in the smoke at the vent.

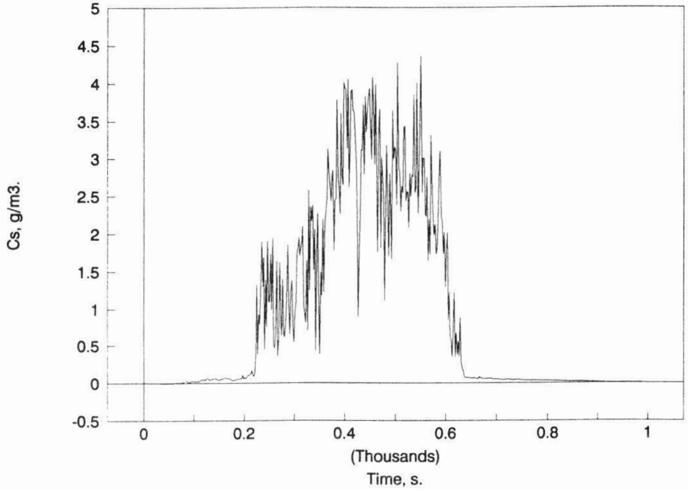

Figure 7. Test 25, derived soot concentrations in the smoke in the vent.

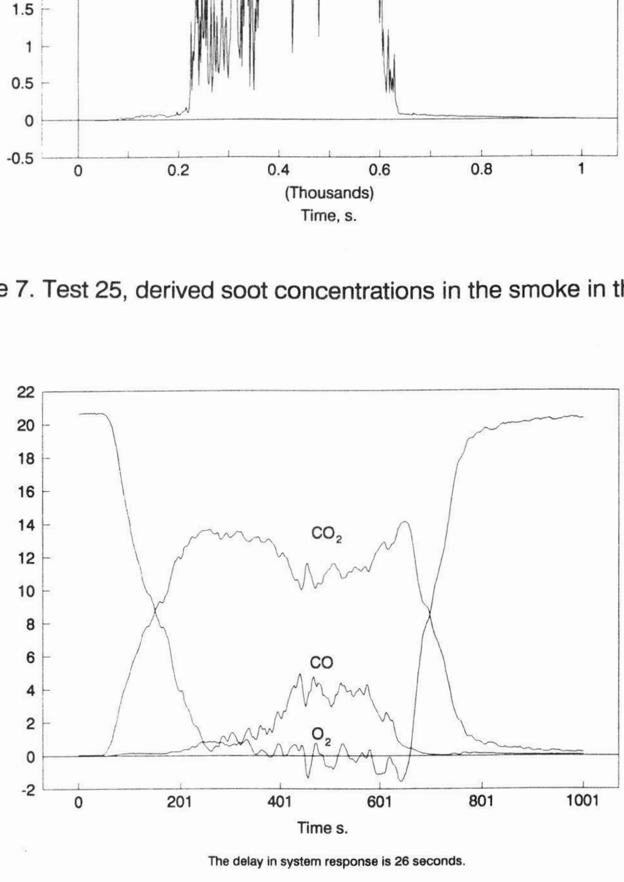

Figure 8. test 25, gas concentrations in the smoke at the vent.

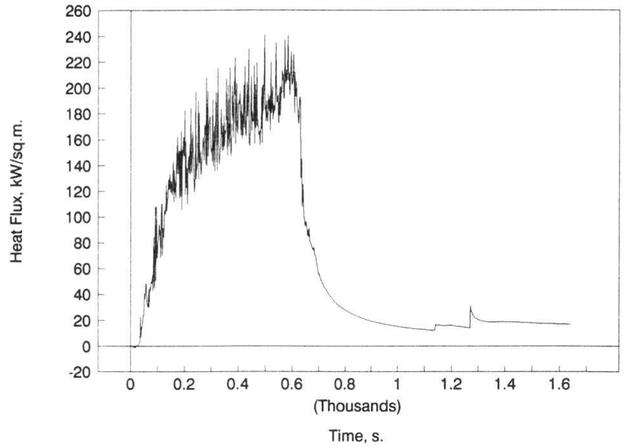

Figure 9. Test 25, radiative heat flux at the ceiling, directly above the pool.

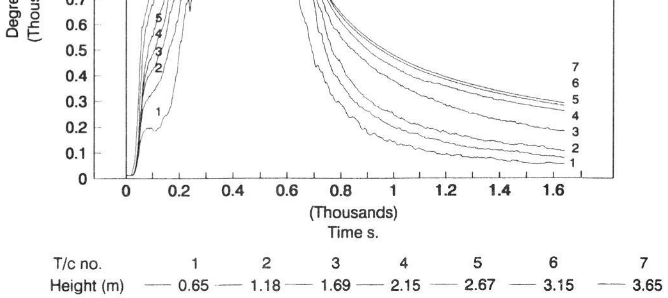

Figure 10. Test 25, temperature at east thermocouple string.

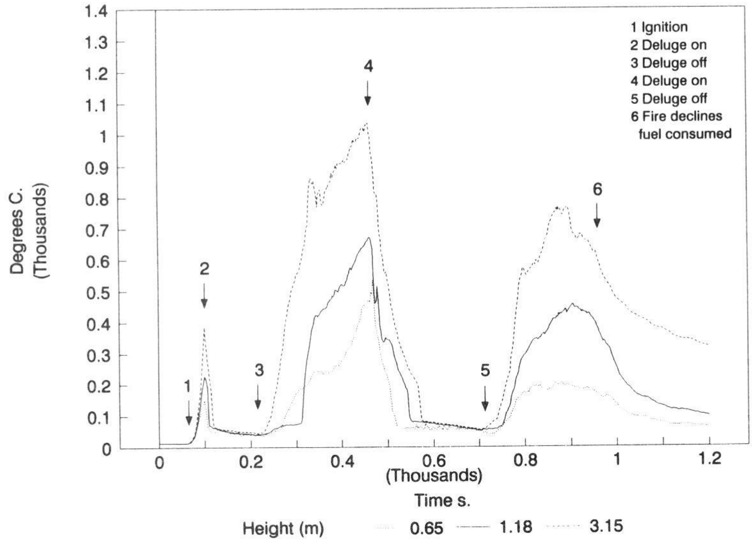

Figure 11. Test 26.
Temperatures at east thermocouple string.

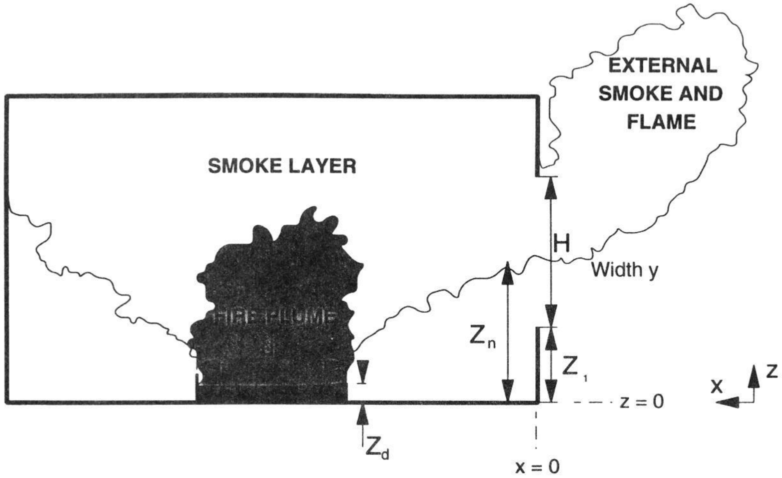

Figure 12. Definition of module and pool geometry.